

Time-dependence of Salinity in Monsoonal Estuaries

V. Vijith, D. Sundar, and S.R. Shetye*

National Institute of Oceanography (CSIR)

Dona Paula, Goa 403 004, India

*Corresponding author.

E-mail address: vvijith@nio.org

Telephone numbers: +919421747872 (mobile), +918322450400 (office)

Abstract

The theories and classification schemes commonly used for understanding estuarine dynamics often refer to a steady state of the estuary in which the salinity field is time-independent. In this state salinity-ingress into the estuary due to different process (diffusion, gravity current formation, impact of tidal asymmetries, etc.) is balanced by salinity-egress induced by runoff. Here we point out that the salinity field of the estuaries that are located on the coasts of the Indian subcontinent and come under the influence of the Indian Summer Monsoon (ISM) is never in a steady state. We refer to such estuaries as “monsoonal estuaries”, an example of which is the Mandovi estuary located on the west coast of India. We describe the annual cycle of the salinity field in this estuary and conclude that the essential unsteadiness of the salinity field arises from two features of the runoff into it. First, most of the runoff occurs as a series of episodes of highs and lulls spread over about 4 months of the wet summer monsoon. Second, the total runoff is large, well over an order of magnitude larger than the estuarine volume. We define two parameters to represent these two features, and show that they can be used to distinguish the monsoonal estuaries from others.

Keywords: estuary; salinity; runoff; Indian Summer Monsoon; unsteady state; India.

1. Introduction

The processes that control distribution of salinity in an estuary can be grouped into two classes, salinity-ingress and salinity-egress. The latter is associated with runoff into the estuary. The total salt within the estuary gets reduced as the freshwater brought by the runoff mixes with the estuarine water and leaves the estuary. Salinity-ingress, which leads to increase of salinity in the estuary, arises from the following processes: horizontal diffusion, gravity current formation and impact of spring-neap tidal asymmetry, and tidal straining or impact of ebb-flood tidal asymmetry. (Stacey et al., 2001, provide an overview of the last two processes.) When the magnitude of salinity-ingress is equal to that of salinity-egress, the estuary attains a steady-state. Observations have shown that many estuaries do exhibit such a balance, at least approximately. This time-independence, or steady-state, has been the hallmark of many estuarine theoretical frameworks and classification schemes. An example is the well-known and time-proven estuarine model given by Hansen and Rattray (1965 and 1966).

There are, of course, many estuaries that do not always have a balance between salinity-ingress and egress. Often such an imbalance arises due to time-dependence in the freshwater runoff into the estuary. Another possibility, though less frequently documented in literature, is change in the boundary condition at the mouth of the estuary, as shown by Banas et al. (2004). To take into account the time-dependent salinity field in an estuary, Kranenburg (1986) estimated a time scale for the salinity to adapt to a new river-flow condition in well-mixed estuaries. MacCready (1999) extended this study to stratified and partially-mixed estuaries. MacCready (2007) added temporal evolution to the Hansen-Rattray equations to study the variation in salt intrusion length and adjustment time.

The purpose of this paper is to point out that the estuaries that come under the influence of Indian Summer Monsoon (ISM) cannot be treated as being in a steady state *at any time*. These estuaries are located along the coastline of the Indian subcontinent, and their *essential unsteadiness* arises from the characteristics of runoff into them. The runoff is very high during the wet season, the ISM, which usually occurs during June–September. This high runoff is followed by little runoff during the rest of the year, the dry season. Most of these estuaries are shallow, with depth at the mouth of the of 10 m and at the head of the order of a meter. They are convergent, i. e. the width decreases rapidly from mouth to head. Width at the mouth is typically few kilometres and at the head is about a tenth of a kilometre. These estuaries are partially mixed during the dry season. We refer to such estuaries as “monsoonal estuaries” following earlier usage (see, for example,

Khadkikar, 2008). To make a case for essential unsteadiness of the salinity field in a monsoonal estuary, we use the Mandovi estuary on the west coast of India as an example. In Section 2, we describe the annual cycle of the salinity field in this estuary. In section 3, we discuss how the salinity balance in the estuary differs from that in a steady-state estuary. In Section 4, we identify key parameters, related to runoff into the estuary, that distinguish monsoonal estuaries from others. Section 5 summarizes our conclusions.

2. Variation of salinity in the Mandovi Estuary

The Mandovi estuary is located on the coastal plain between the central west coast of India (inset, Figure 1) and the Sahyadri range (also known as the Western Ghats) in the state of Goa. The Mandovi is one of the two major estuaries of this state. The other, Zuari estuary, is connected to the Mandovi through a channel (Figure 1). The channel, however, is too narrow to make a significant impact on the dynamics of either estuary or on the exchange of mass. We therefore treat the Mandovi as an independent estuary. Table 1 summarizes its major physical characteristics. An overview of the present understanding of the estuary is available in Shetye et al. (2007a). Tides in the Mandovi are mixed, semi-diurnal dominant (Sundar and Shetye, 2005).

A number of rivers join the estuary along the length of its channel, while rivers Mhadei and Ragda join it at the upstream end. These rivers bring freshwater to the estuary during the rainy season, i.e., during the ISM (usually June–September). At this time, moisture-laden westerly winds blow on to the central west coast of India. As the air rises, making its way eastward while going over the Sahyadris, the topographic influence leads to high rainfall (Rao, 1976) in the catchment area of the rivers that feed the Mandovi. This monsoonal precipitation has spikes of high rainfall during active spells of the monsoon. There are lulls during breaks or weak spells in the monsoon. A typical pattern of daily runoff in the region is shown in Figure 2, which presents the data collected during the ISM of 1992. The gauge that recorded these data was located near the head of the estuary. With a number of rivers, rivulets, and streams bringing runoff to the Mandovi, it has been estimated that the runoff entering the estuary doubles from head to mouth (Suprit and Shankar, 2008). The runoff is high following an episode of high precipitation over the catchment area of rivers that feed the estuary.

Consider the runoff during one of the days shown in the record in Figure 2. On 26 July 1992, the runoff at the head was $1946 \text{ m}^3 \text{ s}^{-1}$, which is equivalent to $168 \times 10^6 \text{ m}^3 \text{ day}^{-1}$. The volume of the

Mandovi estuary is $160 \times 10^6 \text{ m}^3$. Hence, even if no other river had brought any runoff to the estuary on 26 July 1992, the runoff brought by the Mhadei on that day was enough to flush the entire main channel of the Mandovi and fill it with freshwater: the estuary would have turned into a river on that day. When runoff brought by other rivers is taken into account, the description of the estuary as a river during episodes of high runoff becomes even more apt. Such episodes of high runoff, however, are few, and occurred only once in 1992, as seen in Figure 2. Nonetheless, their contribution to the total seasonal runoff during the ISM is significant. During June–September of 1992, the volume of runoff at the upstream end was $3100 \times 10^6 \text{ m}^3$, i. e. 19.4 times the volume of the estuary. Taking into account the estimate that the runoff at the mouth is roughly two times that at the head, the total seasonal runoff into the estuary is approximately 40 times the volume of the estuary. With this volume of runoff, it is expected that the estuary gets flushed many times over during the ISM.

Following withdrawal of the ISM, which usually occurs during October, runoff into the Mandovi decreases rapidly. According to Shetye et al. (2007a), the average runoff during the dry season (November–May) is only 3.4% of the annual average. Data collected during 1979–99 show that the monthly average runoff at the head of the Mandovi estuary during the months of January–May was $3.9 (\pm 1.7)$, $1.8 (\pm 0.7)$, $0.8 (\pm 0.7)$, $0.4 (\pm 0.7)$ and $0.5 (\pm 1.3) \text{ m}^3 \text{ s}^{-1}$ respectively. These values correspond to monthly runoff of $10.4 (\pm 4.5)$, $4.4 (\pm 1.7)$, $2.1 (\pm 1.9)$, $1.0 (\pm 1.8)$ and $1.3 (\pm 3.4) \times 10^6 \text{ m}^3$ respectively, during January–May.

As runoff decreases, the salinity in the estuary migrates upstream. During the seven-month-long dry season (November–May), salinity in the estuary keeps increasing. Figure 3 shows how the salinity field in the estuary changes during a year. It is based on salinity sections that were collected along the main channel of the estuary, roughly once every two weeks, during a year starting 1 June 2007. The sections were made by using data collected with a portable SeaBird CTD (SBE 19 plus) from a boat that steamed from the mouth towards the head in the main channel of the estuary. The boat stopped at predetermined locations to collect a vertical CTD profile from surface to the bottom at the mid-channel location as far as possible. It took approximately 4 to 5 hours to complete a section. Similarly, a section was made using data collected when the boat steamed from the upstream end to the mouth. Differences between the two sections were found to be minor. The data collected while moving upstream were used in Figure 3.

The section shown in Figure 3(a) was collected on 1 June 2007. The ISM had still not set in that

year on this day. Hence, the section shows a salinity field that is typical of what is observed at the end of the dry season. Salinity as high as 35.5 was observed at a distance of 6 km from the mouth of the estuary. (Throughout this paper, salinity is reported in the practical salinity scale.) As the monsoon set in, the runoff into the estuary picked up and salinity in the estuary decreased. Figure 4(a), which shows daily rainfall at Panaji near mouth of the estuary, allows us to appreciate how the monsoon rainfall evolved that year. On 10 August 2007, there was hardly any saline water in the estuary (Figure 3(b)), i.e., the estuary was more like a river that day. Two weeks later, on 24 August 2007, following a lull in the rainfall, salinity intruded into the estuary. The salinity structure at this time, as seen in Figure 3(c), is reminiscent of that found in salt-wedge estuaries. During the ISM, the salinity field in the estuary often oscillates between the field seen in Figure 3(b) and that in Figure 3(c). When runoff is high, the salinity field is like that in Figure 3(b). When runoff weakens, the field is more like Figure 3(c). By 19 October 2007, the ISM was in a phase of withdrawal. As a result, the runoff decreased, and the salinity intruded farther in the estuarine channel, as seen in Figure 3(d). The salinity field still retained characteristics of a salt wedge at this time.

After the withdrawal of the ISM in 2007, and with the onset of the dry season, runoff in the estuary dropped rapidly. With it, the character of the salinity field changed from a salt wedge to partially mixed. This change can be seen by comparing Figure 3(d), which shows the salinity field as the monsoon withdrew, with Figure 3(e), which shows the salinity field on 11 January 2008. Runoff into the estuary weakened and salinity intrusion continued as the dry season progressed. Shetye et al. (2007b) have noted that the process of intrusion of salt at this time is typical of the process found in partially-mixed estuaries, with vertical salinity stratification much better developed during neap tides in comparison to spring tides. As the dry season approached its end, a salinity of about 3.6 is found at a distance of 41 km from the mouth. This situation is seen in the section collected on 16 May 2008 (Figure 3(f)). This section is similar to that seen in Figure 3(a).

Figure 3 shows that from the point of view of salinity evolution, there are two distinct seasons: a shorter wet season of about 4–5 months; and a dry season of about 7–8 months. During the wet season the salinity field changes rapidly in response to variation in runoff. Whenever there is significant salinity intrusion owing to reduced runoff, the salinity distribution takes the shape of a salt wedge. During the dry season, the salinity behaves like that in a partially-mixed estuary. With runoff weakening, salinity intrusion keeps increasing throughout the dry season. In essence, a distinct feature of the annual evolution of salinity in the Mandovi estuary is that the estuary is *never*

in a steady state.

Figure 3 documents well how the salinity field changes with saline water creeping into the estuary slowly, but persistently, during the dry season. It does not, however, do justice to the rapid changes that can occur in the salinity field due to the impact of high rainfall and resulting high runoff. This change can occur from day to day. In order to appreciate such changes, the following observations were made during 2007–2008 in the Mandovi. Every day, at 1100 hours local time, a vertical profile was collected at a point located in the middle of the estuarine channel at a distance of 7 km from the mouth (near the city of Panaji). The observation point is marked with “X” in Figure 1. Figure 4(b) and (c) have been prepared using these profiles. The former shows salinity at the surface and the latter at a depth of 5 m. These two figures, together with Figure 4(a), which shows daily precipitation at Panaji, reveal the changes that can occur from day to day when an event of high rainfall occurs in the region. The figure also shows how, during a lull in the monsoon, salinity creeps into the estuary. Such increases and decreases in salinity occur throughout the wet season. We note that with the observations in Figure 4(b) and (c) made at a fixed time, the figures would have problems related to aliasing with tidal oscillations. Nevertheless, these problems do not prevent us from drawing our two conclusions: rapid changes occur during the wet season, and slow, but persistent, increase occurs during the dry season. The oscillations in salinity during the dry season are due to differences in tidal excursion during springs and neaps.

The Mandovi is used extensively for navigation. As a result, direct current observations with moorings are not allowed. Hence, the database on current-meter observations is weak. The meagre data that exist suggest that the peak tidal velocity during spring tide is of the order of 0.8 m s^{-1} . We expect this value to vary with location, but, in the absence of suitable data, we assume it to be representative of peak tidal velocity during springs everywhere. Semi-diurnal tides are dominant in the estuary. Hence, we expect the tidal excursion to be about 10 km, or one-fifth the length of the estuary. In Figure 5, we estimate runoff-induced velocity for three different runoff values at the head of the estuary. These values are chosen to represent very high ($1000 \text{ m}^3 \text{ s}^{-1}$), high ($500 \text{ m}^3 \text{ s}^{-1}$) and moderate ($100 \text{ m}^3 \text{ s}^{-1}$) runoff events during the ISM. Runoff at every 2 km from the head to the mouth is calculated using the model results of Suprit and Shankar, (2008). Runoff-induced velocity is then obtained from these runoffs by dividing it by the area of cross-section. This area of cross-section, measured with respect to mean sea level, is kept constant with time. Figure 5 shows the supremacy of runoff-induced velocity over tidal-induced velocity during very-high- and high-runoff events. Tide competes with runoff to determine the velocity field during high-runoff to moderate-

runoff events. Tidal-induced velocity dominates during the dry season when runoff is weak.

We conclude this section by estimating the flushing time of the Mandovi, and by examining its implications. Flushing time is the time required to renew existing volume (V_e) of water in an estuary at a volumetric flow rate (Q) through the estuary (Monsen et al., 2002), i.e.,

$$T_f = \frac{V_e}{Q} . \quad (1)$$

Volumetric flow rate through an estuary is controlled by two processes. The first is new riverine water entering the estuary as runoff, and the second is new seawater entering the estuary at its mouth during floods. If we assume that flushing is due to river runoff (Q_R) alone, then runoff induced flushing time, T_{fR} , is given by,

$$T_{fR} = \frac{V_e}{Q_R} . \quad (2)$$

When runoff in the Mandovi is as high as $2000 \text{ m}^3 \text{ s}^{-1}$, T_{fR} is as small as 0.9 day. Climatological value of monthly mean runoff into the Mandovi during June–September varies between $227 \text{ m}^3 \text{ s}^{-1}$ and $967 \text{ m}^3 \text{ s}^{-1}$; T_{fR} during these months are 8.2, 1.9, 2.3 and 7.1 days for June–September, respectively. Beyond the ISM, as runoff decreases, T_{fR} increases. During the dry season, when runoff is weak, tide is expected to play a dominant role in flushing of the Mandovi with seawater. Flushing time under such circumstances can be calculated using the method of tidal prism (Dyer 1997; Monsen et al., 2002). In this case the tide driven flushing time (T_{fT}) is given by,

$$T_{fT} = \frac{V_e T}{\square - b \square P} , \quad (3)$$

where, T is the tidal period, P is the tidal prism, and b is the return flow factor (Monsen et al., 2002). For the Mandovi, the tidal prism is estimated at $66.5 \times 10^6 \text{ m}^3$, and semi-diurnal period (12.42 hours) is the predominant tidal period. Return flow factor (b) is the fraction of ebb water returning to the estuary during the subsequent flood tide. We set b to 0.5 following SCCC (1985); USEPA (1985). The tide-driven flushing time (T_{fT}) is then 2.5 days.

This implies that the time scale of approach to equilibrium is of the order of days during the dry season. The fact that the salinity increases at a much slower rate in the Mandovi means that while runoff during the dry season is much weaker than that during the wet season, whatever freshwater influx that occurs into the estuary is sufficient to keep the salinity close to zero at the upstream end.

Helping this is the fact that the estuarine channel at the upstream end is narrower and shallower than the channel farther downstream. As a result, volume of the 20 km section of the channel at the upstream end is $\sim 10 \times 10^6 \text{ m}^3$ i. e. less than 1% of the volume of the estuary (Table 1). As a consequence, the little runoff that enters the estuary is enough to keep the salinity at the upstream end close to zero throughout the dry season of well over six months even though the flushing time of the estuary is less than 3 days.

3. Salt balance in the Mandovi Estuary

The above discussion reveals two characteristics of the salinity field in the Mandovi estuary. First, the field is quasi-periodic with a period of about a year. The periodicity, rather the quasi-periodicity, is ensured by the fact that runoff during the ISM is high enough so that the estuary is completely filled with freshwater at least a few times. Second, after the withdrawal of the ISM, runoff is weak and keeps decreasing throughout the dry season. This ensures a monotonic increase in salinity (averaged over a tidal period) during the nearly seven-month-long dry season.

In Section 1, we have noted that salt balance in an estuary is determined by two processes, salinity-ingress and runoff-induced salinity-egress. We can therefore write that at a point in the estuary,

Rate of change of salinity = contribution of salinity-egress + contribution of salinity-ingress.

We represent this relationship schematically in Figure 6. Whenever salinity-ingress is larger (smaller) than egress at a location in the estuary, salinity increases (decreases) at that location. When the two are in balance all the time at all locations, the rate of change of salinity vanishes, and the state of the salinity variation at any time at all locations occupies a point in the (x,y) plane in the figure. This is the situation depicted in the Hansen-Rattray model. The Mandovi estuary, by not being in a steady state at any time of the year, never occupies this plane. Once runoff decreases to low values during the dry season, salinity-egress decreases significantly, and salinity increases due to salinity-ingress. This state of salinity variation at a location in the estuary is represented by a point that is close to the (y,z) plane in the figure. The point will not lie exactly on the (y,z) plane because, as noted in the concluding part of the previous section, there is some salinity-egress, particularly at the upstream end of the estuary, that occurs throughout the dry season. When runoff is very high during the rainy season, salinity variation at a location in the estuary will be dominated by runoff-induced salinity-egress. The state of such a location occupies a point in the (x,z) plane in the figure. During lulls in runoff, at a location in the estuary, both salinity-egress and processes responsible for salinity-ingress contribute. As a result, the state of salinity variation at that location

would occupy a point somewhere in the (x,y,z) space in the figure.

4. Comparison with other estuaries

While the phrase 'monsoonal estuaries' has been used to describe Indian estuaries, the meaning of the phrase has not been elucidated. In this section, we identify two parameters that distinguish these estuaries. These parameters follow from the two distinguishing characteristics of runoff into the estuaries. First, the monsoonal estuaries experience total annual runoff that is many times estuarine volume. Second, there is a high “peakiness” or seasonality in the runoff.

The first of the two parameters is the ratio of volume of total annual runoff to volume of the estuary:

$$\eta_R = \frac{R_a}{V_e}, \quad (4)$$

where, R_a is the volume of total annual runoff (m^3) and V_e is the volume (m^3) with respect to mean sea level in the estuary. Higher the value of η_R , higher is the runoff. As noted earlier, this parameter is ~ 40 for the Mandovi. Higher the value, greater is the chance that the estuary turns 'fresh' at some time(s) during the wet season.

The second parameter we define is,

$$\eta_T = \frac{\text{Maximum monthly runoff}}{\text{Mean monthly runoff}}. \quad (5)$$

Here the right hand side is computed from the twelve monthly values of the climatology of the runoff into an estuary. η_T depends on the temporal evolution of runoff during the year. For a runoff that does not change from month to month, $\eta_T = 1$. This is the minimum value that η_T can take. Shorter the wet season (with higher runoff) and higher the value of runoff during a month of this season (in comparison to the average over the year), greater is the value of η_T . For the Mandovi, $\eta_T \sim 5$.

We now compare values of the above two parameters for ten better known partially-mixed estuaries of the world with those for the Mandovi and three other monsoonal estuaries along the coast of India. Table 2 lists all the 14 estuaries. The table also lists the sources that have been used to compute η_R and η_T for each estuary. Figure 7 shows locations of the estuaries and Figure 8 the annual cycle of monthly runoff in these estuaries. Using the runoff and the values of estuarine

volumes given in Table 2, we have computed η_R and η_T for each of the 14 estuaries listed in the table. Values for each estuary are then depicted in a plot of η_R versus η_T in Figure 9.

In the figure, each of the four monsoonal estuaries appears in the shaded area for which $\eta_T > 2$ and $\eta_R > 10$. The estuaries in this area have high annual runoff and a distinctly higher runoff during the wet season as compared to the dry season. There are estuaries that have either high runoff (Columbia River Estuary, for example) with $\eta_R > 10$, or have high variation in runoff with season ($\eta_T > 2$ for Ria of Ferrol, Willapa Bay, and San Francisco Bay, for example). Among the fourteen estuaries considered in the present study, it is only for monsoonal estuaries that both parameters have high values. When either one of these parameters is low, it is possible to have the salinity field in a steady state. When η_R is high, but η_T is low, a steady state is possible because runoff does not change significantly from month to month. When η_R is low, but η_T is high, the magnitude of runoff is not sufficiently high to have a significant impact on the variation of salinity. In either of these two situations, it is expected that amplitude of salinity variation will never be as high as the 35 that is observed near the mouth in monsoonal estuaries like the Mandovi.

5. Concluding Comments

Using the Mandovi estuary as an example, we have shown that the salinity field in a monsoonal estuary is never in a steady state. The unsteadiness arises because of two features of runoff. First, the total runoff is high and the volume of freshwater brought by the runoff is well over an order of magnitude higher than the volume of the estuary. Second, the runoff is high during the summer monsoon. During this time, there are at least a few episodes of high in runoff. During these episodes, the entire estuary is filled with freshwater, and therefore turns into a river. The runoff highs are followed by lulls. During the latter, there is competition between runoff-induced salinity-egress and salinity-ingress by the usual estuarine processes. This competition results in rapid change in salinity.

During the dry season salinity intrudes in the upstream direction. However, there is enough runoff to ensure that the salinity at the upstream end is close to zero all the time. Helping to ensure this is the geometry of the estuary. Like the Mandovi, most estuarine channels located along the Indian coast are convergent in nature. Their narrowness at the upstream end helps to keep the salinity near zero even though the runoff keeps decreasing until onset of the next ISM.

It is expected that behaviour similar to that found in Indian monsoonal estuaries is also observed in other areas that have marked seasonality in runoff, such as other parts of Asia that experience a monsoon climate, tropical South America, and parts of Australia and South Africa. These characteristics could also be found in regions where the source of runoff could be melting of ice rather than rainfall. In all these estuaries, unsteady behaviour of the salinity field is an essential feature. Models built to understand them must take into account this unsteadiness at a fundamental level. Monsoonal and other similar estuaries provide a good ground for testing the models that take unsteady behaviour into account (see Section 1). Future research should include such tests.

There is another aspect that needs to be researched. This aspect is related to the residence time of water (Monsen et al., 2002) in monsoonal estuaries. It is clear that the residence time of a parcel of freshwater that enters the estuary will differ considerably between the wet summer monsoon and the longer dry season. The residence time will also differ with the location where the parcel enters the estuary. Such variations are expected to have an impact on the ecosystems that are found in such estuaries. There are virtually no studies that have addressed this issue in the monsoonal estuaries of India. Future research will need to enlarge our understanding of these systems.

Acknowledgements

V. Vijith acknowledges the financial support from Council of Scientific and Industrial Research, India. We thank the team that collected the year-long Mandovi dataset during 2007–2008, and helped in subsequent analysis. Comments from the anonymous reviewers helped to improve the manuscript considerably. This is NIO contribution XXXX.

References

- Attrill, M.J., Power, M., 2000. Modelling the effect of drought on estuarine water quality. *Water Research*, 34 (5), 1584-1594.
- Banas, N.S., Hickey, B.M., MacCready P., 2004. Dynamics of Willapa bay, Washington: A highly unsteady, partially mixed estuary. *Journal of Physical Oceanography*, 34, 2413-2427.
- Cheng, R.T., Casulli, V., Gartner, J.W., 1993. Tidal, Residual, Intertidal Mudflat (TRIM) model and its applications to San Francisco Bay, California. *Estuarine, Coastal and Shelf Science*, 36, 235-280.
- Cook, T.L., Sommerfield, C.K., Wong, K.-C., 2007. Observations of tidal and springtime sediment transport in the upper Delaware estuary. *Estuarine, Coastal and Shelf Science*, 72, 235-246.
- deCastro, M., Gomez-Gesteira, M., Prego, R., Alvarez, I., 2004. Ria-ocean exchange driven by tides in the Ria of Ferrol (NW Spain). *Estuarine, Coastal and Shelf Science*, 61, 15-24.
- de Jonge, V.N., 1988. The abiotic environment. In: Baretta, J., Ruardij, P. (Ed.), *Tidal flat estuaries: Simulation and analysis of the Ems estuary*. Springer-Verlag, pp. 14-27.
- Dyer, K.R., 1997. *Estuaries: A physical introduction*. 2nd ed. John Wiley, 195 pp.
- Filardo, M.J., Dunstan, W.M., 1985. Hydrodynamic control of phytoplankton in low salinity waters of the James River estuary, Virginia, U.S.A. *Estuarine, Coastal and Shelf Science*, 21, 653-667.
- Ford, M., Wang, J., Cheng, R.T., 1990. Predicting the vertical structure of tidal current and salinity in San Francisco Bay, California. *Water Resources Research*, 26 (5), 1027-1045.
- Godfrey, J.S., 1980. A numerical model of the James River estuary, Virginia, U.S.A. *Estuarine, Coastal and Shelf Science*, II, 295-310.
- Goodrich, D.M., 1988. On meteorologically induced flushing in three U.S. east coast estuaries. *Estuarine, Coastal and Shelf Science*, 26, 111-121.
- Grabemann, I., Uncles, R.J., Krause, G., Stephens, J.A., 1997. Behaviour of turbidity maxima in the Tamar (U.K.) and Weser (F.R.G.) estuaries. *Estuarine, Coastal and Shelf Science*, 45, 235-246.
- Hansen, D.V., Rattray M., 1965. Gravitational circulation in straits and estuaries. *Journal of Marine Research*, 23, 104-122.
- Hansen, D.V., Rattray, M., 1966. New dimensions in estuary classification. *Limnology and Oceanography*, 11(3), 319-326.
- Khadkikar, A.S., 2008. Anatomy of a macrotidal monsoonal estuary, *Geophysical Research Abstracts*, Vol. 10, EGU2008-A-01256, SRef-ID: 1607-7962/gra/EGU2008-A-01256, EGU General Assembly 2008.
- Kranenburg, C., 1986. A time scale for long-term salt intrusion in well-mixed estuaries. *Journal of Physical Oceanography*, 16, 1329-1331.

- MacCready, P., 1999. Estuarine adjustment to changes in river flow and tidal mixing. *Journal of Physical Oceanography*, 29, 708-726.
- MacCready, P., 2007. Estuarine adjustment. *Journal of Physical Oceanography*, 37, 2133-2145.
- Miller, A.E.J., 1999. Seasonal investigations of dissolved organic carbon dynamics in the Tamar estuary, U.K. *Estuarine, Coastal and Shelf Science*, 49, 891-908.
- Monsen, N.E., Cloren, J.E., Lucas L.V., Monismith, S.G., 2002. A comment on the use of flushing time, residence time and age as transport time scales. *Limnology and Oceanography*, 47, 1545-1553.
- Moran, M.A., Limburg, K.E., 1986. The Hudson river ecosystem. In: Limburg, K.E., Moran, M.A., McDowell, W.H. (Ed.), *The Hudson river ecosystem*. Springer-Verlag, pp. 6-39.
- Rao, Y.P., 1976. Southwest Monsoon. *India Meteorological Monograph (Synoptic Meteorology)*, No. 1/1976, Delhi, 376 pp.
- Sharp, J.H., Cifuentes, L.A., Coffin, R.B., Pennock, J.R., Wong, K.-C., 1986. The influence of river variability on the circulation, chemistry, and microbiology of the Delaware estuary. *Estuaries*, 9(4a), 261-269.
- Sherwood, C.R., Jay, D.A., Harvey, R.B., Hamilton, P., Simenstad, C.A., 1990. Historical changes in the Columbia River estuary. *Progress in Oceanography*, 25, 299-352.
- Shetye, S.R., Dileep Kumar, M., Shankar, D., (Ed.), 2007a. *The Mandovi and Zuari estuaries*. National Institute of Oceanography, Goa, India, 145 pp, available at <http://drs.nio.org/drs/handle/2264/1032>.
- Shetye, S.R., Michael, G.S., Pradnya Vishwas, C., 2007b. Mixing and intrusion of salt. In: Shetye, S.R., Dileep Kumar, M., Shankar, D., (Ed.), *The Mandovi and Zuari estuaries*. National Institute of Oceanography, Goa, India, pp. 49-58, available at <http://drs.nio.org/drs/handle/2264/1032>.
- S.C.C.C., 1985. Guidelines for preparation of coastal marina report. South Carolina Coastal Council, Charleston, S.C.
- Stacey, M.T., Burau J., Monismith S.G, 2001. Creation of residual flows in a partially stratified estuary. *Journal of Geophysical Research*, 106, 17013-17037.
- Sundar, D., Shetye, S.R., 2005. Tides in the Mandovi and Zuari estuaries, Goa, west coast of India. *Journal of Earth System Science*, 114 (5), 493-503.
- Suprit, K., Shankar, D., 2008. Resolving the orographic rainfall on the Indian west coast. *International Journal of Climatology*, 28, 643-657.
- U.S.E.P.A., 1985. *Coastal Marinas Assessment Handbook*. United States Environmental Protection Agency, Region IV, Atlanta, Georgia.
- Wood, L.B., 1982. *The restoration of tidal Thames*, Adam Hilger Ltd, Bristol, 202 pp.

Table captions

Table 1: Characteristics of the Mandovi estuary.

Table 2: List of name, location, volume, runoff and references/data sources for the estuaries included in Figures 8 and 9. Volume and monthly runoff for each estuary has been estimated from references/data sources shown in the sixth column. '*' in column 2 indicates that the volume of the estuary has been estimated by integrating area of cross-section given in the references.

Figure captions

Figure 1: The Mandovi estuary located in the state of Goa, west coast of India (inset). Rivers Mhadei and Ragda join the estuary at its upstream end. Other rivers join at other points along the length of the main channel of the Mandovi estuary. Location of Ganjem is shown with a 'filled circle'. Runoff measured at Ganjem is shown in Figure 2. The point marked 'X' in the Mandovi off the town of Panaji gives the location from where time-series shown in Figure 4 were collected.

Figure 2: Runoff ($\text{m}^3 \text{s}^{-1}$) in the Mandovi estuary, measured at head Ganjem (see Figure 1) during the Indian Summer Monsoon of 1992. The horizontal line represents a runoff of $1852 \text{ m}^3 \text{s}^{-1}$ i.e. $160 \times 10^6 \text{ m}^3 \text{ day}^{-1}$.

Figure 3: (a-f) Along channel salinity sections made during a year starting 1 June 2007. The date on which a section was made is shown at the bottom of each figure.

Figure 4: (a) Daily rainfall (mm) at Panaji (see Figure 1 for location). The data were collected from the Indian Meteorological Department observatory at Panaji. (b) Salinity at the surface, and (c) at 5 m depth, at the location shown with 'X' near Panaji in figure 1. Observations cover the period from 1 June 2007 to 5 May 2008.

Figure 5: Estimates of runoff-induced velocities for three different runoff events: very high ($1000 \text{ m}^3 \text{s}^{-1}$), high ($500 \text{ m}^3 \text{s}^{-1}$) and moderate ($100 \text{ m}^3 \text{s}^{-1}$) during ISM. The values in parenthesis denote runoff at the head. Figure 2 helps the reader to appreciate these numbers. The horizontal line represents peak tidal velocity (0.8 m s^{-1}) during spring.

Figure 6: Each of the three terms that determine variation of salinity at a location in an estuary i.e. rate of change of salinity, rate of change of salinity due to runoff-induced salinity-egress and rate of

change of salinity due to salinity-ingress (see Section 3) is represented along an axis of three dimensional space. Every point representing a location in the estuary in the Hansen-Rattray theory lies in the (x,y) plane in the figure. In the monsoonal estuary during the dry season each point in the estuary lies close to the (y,z) plane; during the wet season a point could lie anywhere in the (x,y,z) space.

Figure 7: Locations of the fourteen estuaries listed in Table 1. Annual cycle of runoff of each of these estuaries is plotted in Figure 7. Parameters η_R and η_T (defined in Section 4) for each estuary are plotted in Figure 9.

Figure 8: Mean monthly runoff ($\text{m}^3 \text{s}^{-1}$) in the fourteen estuaries listed in Table 2.

Figure 9: Positions of 14 estuaries around the world on the (η_R , η_T) plane. The monsoonal estuaries occupy the shaded area. Co: Columbia River Estuary; D: Delaware Bay; E: Ems Estuary; F: Ria of Ferrol; H: Hudson River Estuary; J: James River Estuary; S: San Francisco Bay; Ta: Tamar Estuary; T: Thames Estuary; W: Willapa Bay; C: Cochin Backwaters; G: Gautami-Godavari Estuary; M: Mandovi Estuary; Z: Zuari Estuary. For location of the estuaries, see Figure 7.

Length	50 km
Width at the mouth	3.7 km
Width 4 km from the mouth	1.0 km
Width at the head	0.1 km
Depth at the mouth	7 m
Depth at the head	1 m
Volume with respect to mean sea level	$160 \times 10^6 \text{ m}^3$
Tidal prism	$66.5 \times 10^6 \text{ m}^3$
Surface area with respect to mean sea level	35 km^2
Catchment area	1895 km^2
Runoff at the head during June–October	$258 \text{ m}^3 \text{ s}^{-1}$
Runoff at the head during November–May	$6 \text{ m}^3 \text{ s}^{-1}$
Tidal range at the mouth (Spring)	2.3 m
Tidal range at the mouth (Neap)	1.5 m

Table 1

Table 2

Estuary and its location	Volume (10 ⁶ m ³)	Runoff (m ³ s ⁻¹)		References/Data source	Remarks about monthly-mean runoff data used to draw Figures 8 and 9
		Maximum monthly	Mean monthly		
Columbia River estuary, U.S.A. (west coast)	3900	10689.7	7543.1	Sherwood et al. (1990)	Based on data during 1969-1982
Delaware Bay, U.S.A. (east coast)	18900	1126.4	499.6	Cook et al. (2007), Goodrich (1988), Sharp et al. (1986)	Based on data during 1912-2003
Ems estuary, Netherlands (north coast)	1440	175.0	110.3	de Jonge (1988)	Based on data during 1970-1979
Ria of Ferrol, Spain (north-east coast)	250	14.5	6.0	de Castro et al. (2004)	Based on data during 1970-1982
Hudson River estuary, U.S.A. (east coast)	1925*	877.3	376.7	Ralston et al. (2008), Moran and Limburg (1986)	Based on data during 1918-1980
James River estuary, U.S.A. (east coast)	2150*	320.0	155.3	Godfrey (1980), Filardo and Dunstan (1985)	Computed from daily values during 1982
San Francisco Bay, U.S.A. (west coast)	6600	5478.3	1173.4	Cheng et al. (1993), Ford et al. (1990)	Computed from daily values during 1986
Tamar estuary, England (south-west coast)	160	57.0	45.0	Grabemann et al. (1997), Miller (1999)	Figure 8 is based on daily values during Jun. 1988 to Jun. 1989. Figure 9 is based on long-term mean.
Thames estuary, England (east coast)	1350*	125.2	71.1	Attrill and Power, (2000), Wood, (1982).	Based on data during 1977-1988
Willapa Bay, U.S.A. (west coast)	1000*	385.0	135.4	Banas et al. (2004)	Computed from daily values during Aug. 1999 to Aug. 2000
Cochin backwaters, India (west coast)	530	1858.7	706.9	B. Nagesh (Personal Communication), Central Water Commission, India	Based on data during 1978-2001
Goutami-Godavari estuary, India (east coast)	325	3348.5	659.0	M. Dileep Kumar (Personal Communication), Irrigation Department, Andhra Pradesh, India	Computed from daily values during 2007
Mandovi estuary, India (west coast)	160	967.3	206.6	Shetye et al. (2007a), Central Water Commission, India	Based on data during 1979-1999
Zuari estuary, India (west coast)	270	422.5	103.1	Shetye et al. (2007a), Central Water Commission, India	Computed from daily values during 1978

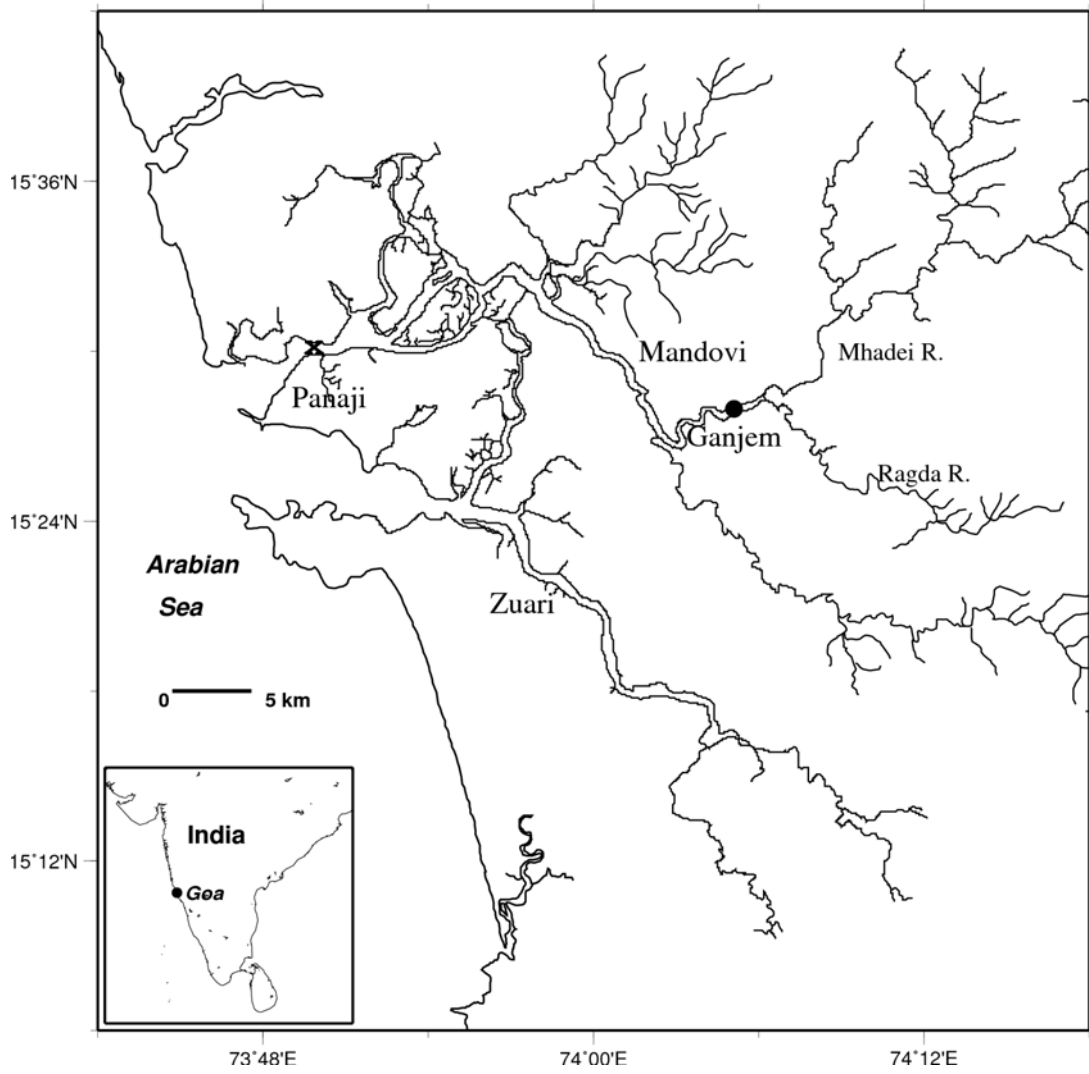


Figure 1

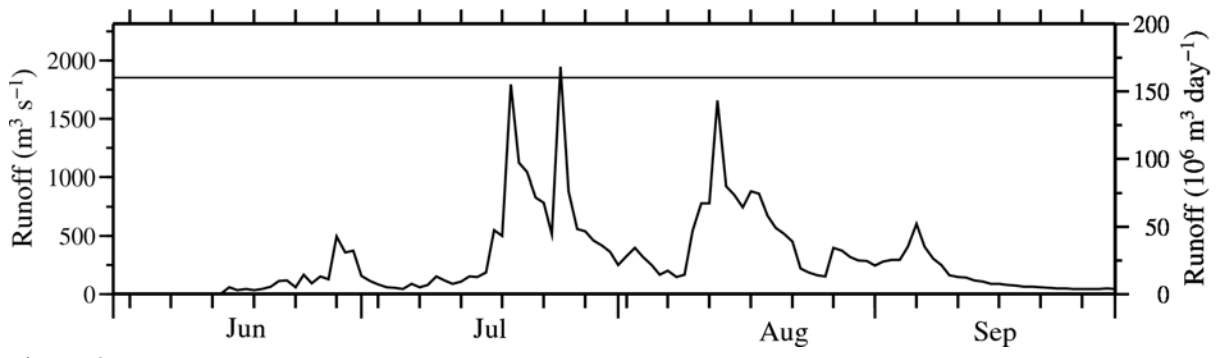


Figure 2

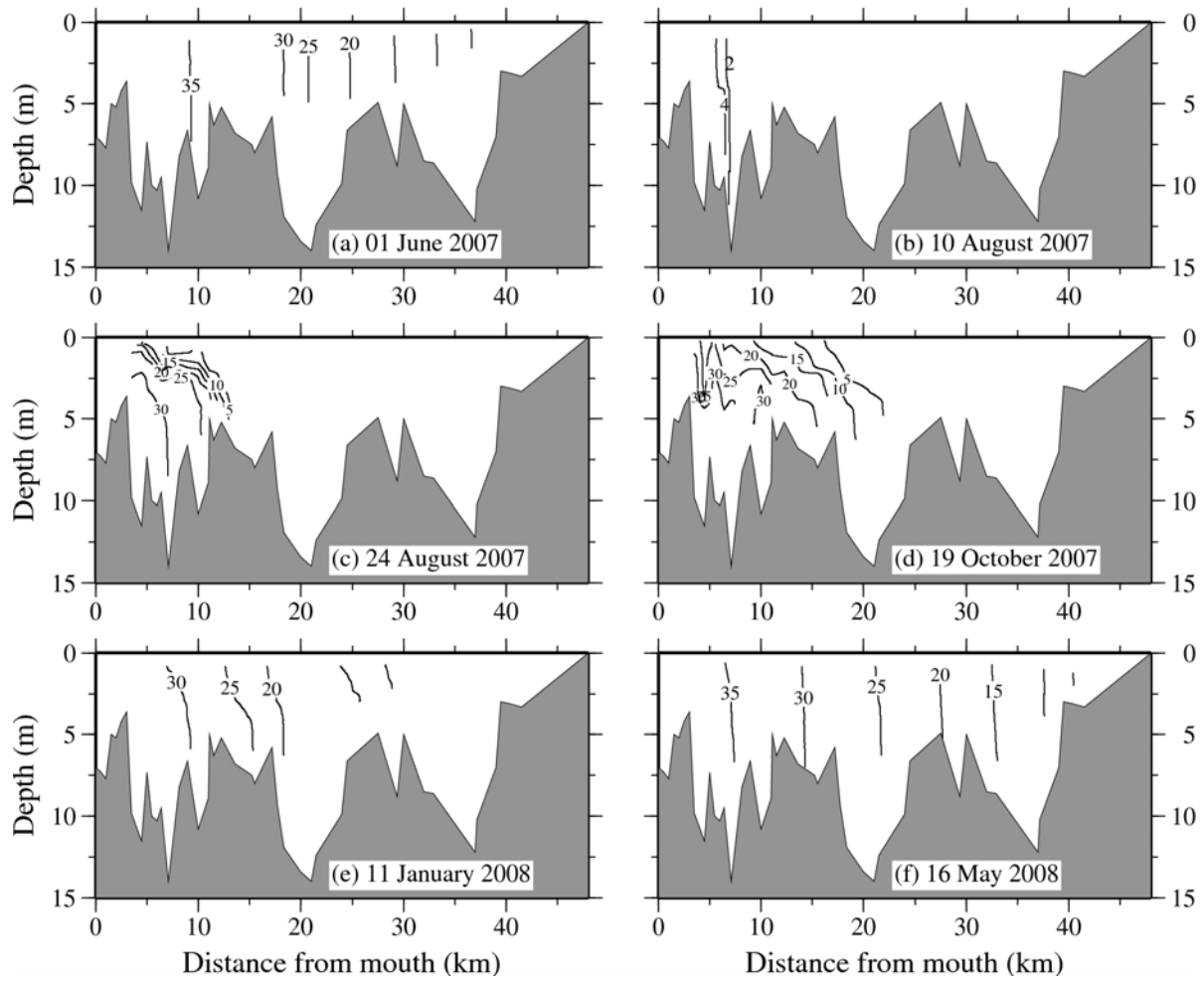


Figure 3

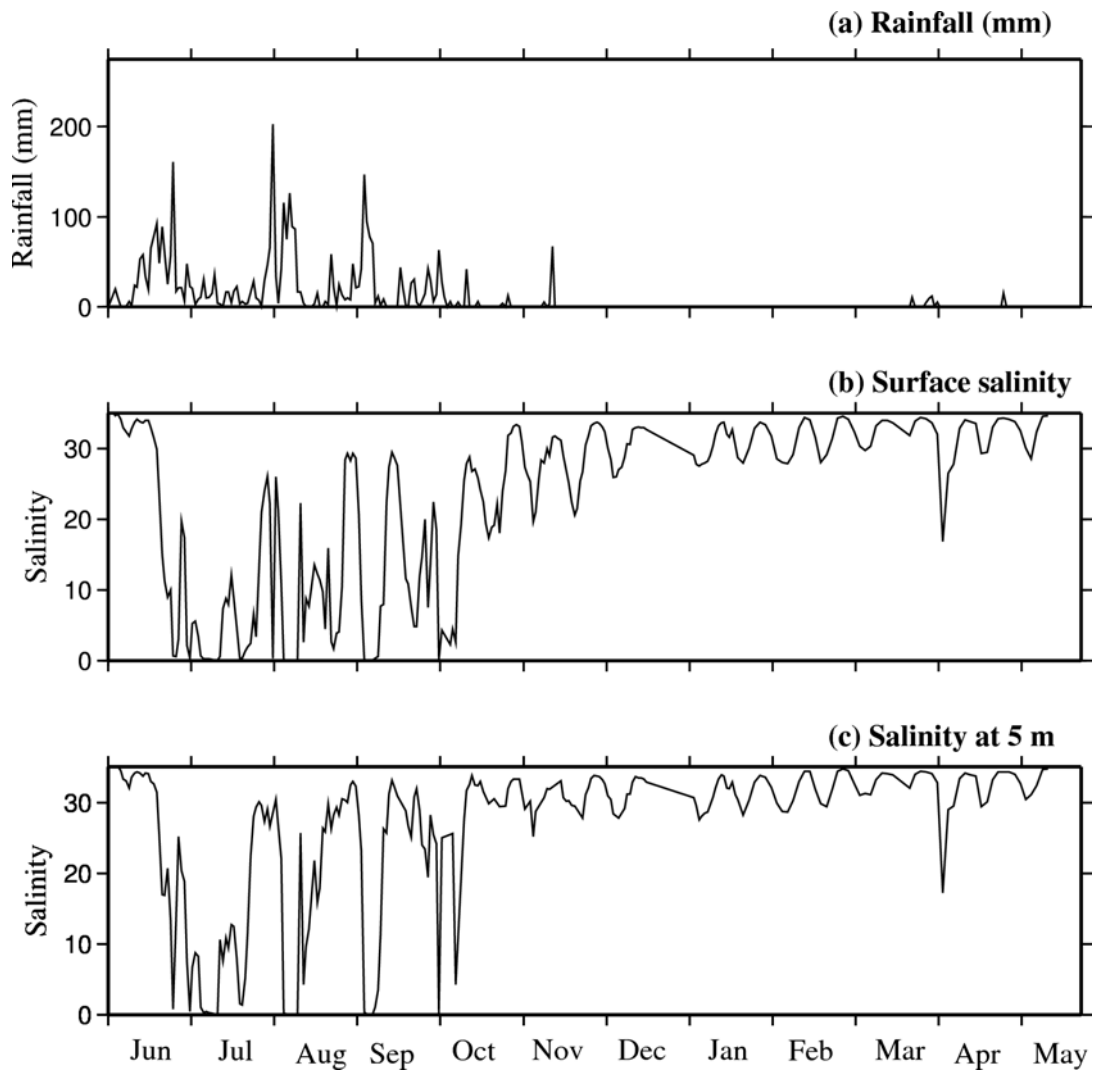
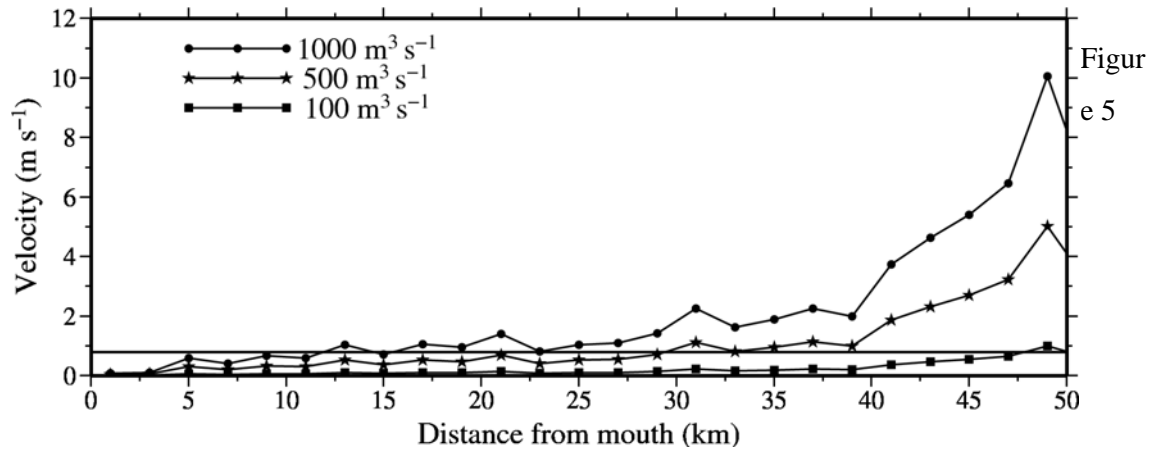


Figure 4



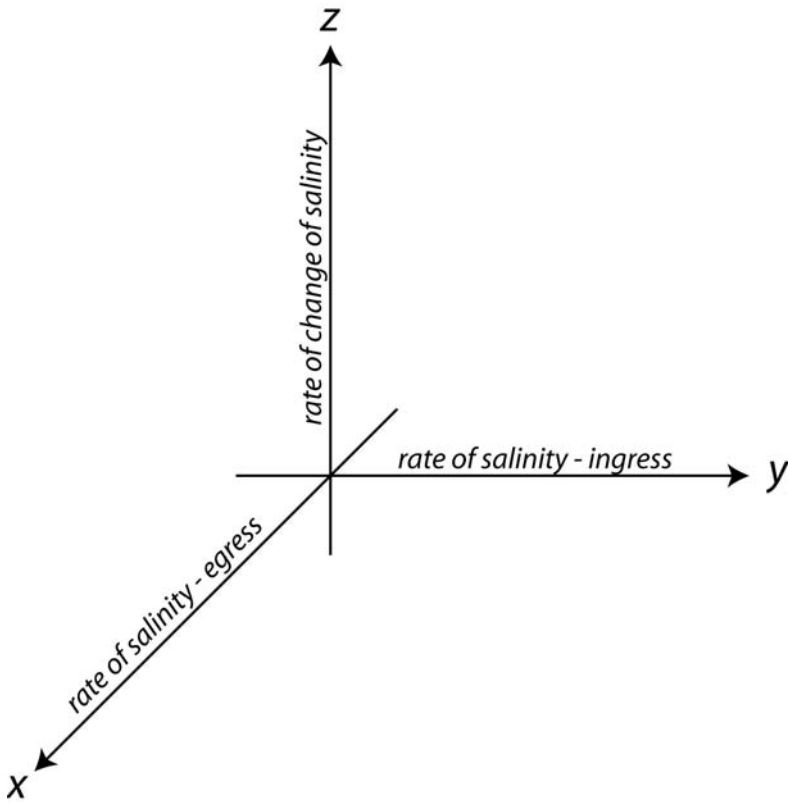


Figure 6

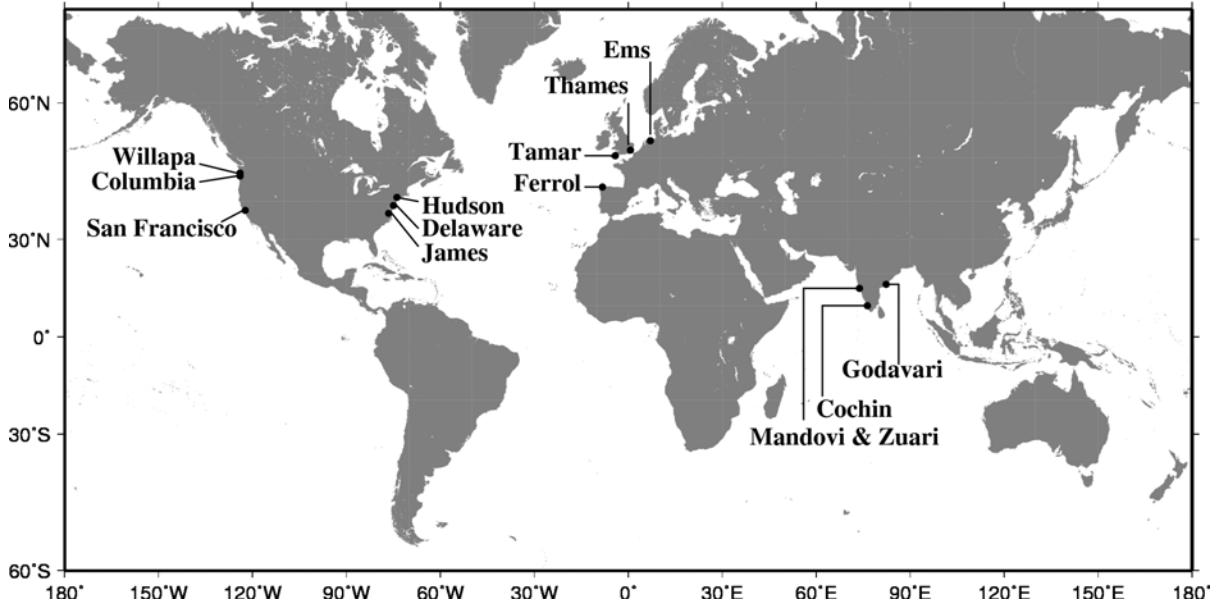


Figure 7

